ELSEVIER

European Journal of Cancer 41 (2005) 635–646

European Journal of Cancer

www.ejconline.com

Imbalance of the mitochondrial pro- and anti-apoptotic mediators in neuroblastoma tumours with unfavourable biology

Frida Abel [a], Rose-Marie Sjöberg [a], Staffan Nilsson [b], Per Kogner [c], Tommy Martinsson [a,*]

[a] *Department of Clinical Genetics, Gothenburg University, Sahlgrenska University Hospital/East, S-416 85 Gothenburg, Sweden*
[b] *Institution of Mathematical Statistics, Chalmers University of Technology, Gothenburg, Sweden*
[c] *Childhood Cancer Research Unit, Karolinska Institutet, Astrid Lindgren Children's Hospital Q6:05, S-171 76 Stockholm, Sweden*

Received 3 August 2004; received in revised form 17 November 2004; accepted 17 December 2004

Abstract

It has been proposed that a lack of apoptosis plays an important role in neuroblastoma (NB) progression. We therefore screened cDNA array filters, including 198 apoptotic genes, in order to identify mRNA transcripts that are differentially expressed in tumours with unfavourable *versus* favourable biology. Twenty-one genes were analysed further using real-time reverse-transcriptase-polymerase chain reaction (RT-PCR). Significantly lower levels of *DNCL1* (PIN; P_c(corrected) = 0.0054) and *NTRK1* (TrkA; P_c = 0.039) were found in NB tumours with unfavourable biology. In addition, *BID*, *BCL2*, *APAF1*, *CASP2*, *CASP3* and *CASP9* were found to be preferentially expressed in tumours with favourable biology, whereas *CDKN1A* (p21), *IL2RA*, and *MCL1*, were found to be preferentially expressed in NB tumours with unfavourable biology. In conclusion, mRNA levels of transcripts encoding pro-apoptotic mediators of the mitochondrial apoptotic pathway were found to be expressed to a lower extent in tumours with unfavourable biology. Our data also suggest that the mitochondrial pathway is suppressed in advanced stages of NB tumours, due to an imbalance between anti-apoptotic and pro-apoptotic mediators which is a finding that may have therapeutic significance.

Keywords: Apaf-1; Caspase*; Mcl-1; LC8; DLC8; Bcl-2

1. Introduction

Neuroblastoma (NB) is a tumour of the sympathetic nervous system with a complex biological heterogeneity depending on the clinical stage and age at diagnosis. Generally, children diagnosed before age one and/or with localised disease are cured with surgery and little or no additional therapy. By contrast, older children, frequently have extensive metastases at diagnosis, and many of them die from tumour progression despite intensive chemotherapy. The most important prognostic marker in determining the treatment for NB patients is amplification of the oncogene *MYCN*, seen in approximately 31% of advanced NBs (reviewed in Ref. [1]). Deletion of chromosome arm 1p and gain of chromosome arm 17q are also of great prognostic importance [2,3].

Although the molecular mechanism underlying spontaneous regression seen in NB tumours with favourable biology is still unclear, it is believed that this process, at least partially, involves factors regulating programmed cell death or apoptosis. Proper regulation of apoptosis is essential for normal homeostasis and tissue development [4,5]. Aberrations in apoptosis may contribute to the pathogenesis of cancer, and are therefore likely to be important in the progression to advanced NB.

* Corresponding author. Tel.: +46 31 343 4803; fax: +46 31 842 160.
E-mail address: Tommy.Martinsson@clingen.gu.se (T. Martinsson).

0959-8049/$ - see front matter © 2005 Elsevier Ltd. All rights reserved.
doi:10.1016/j.ejca.2004.12.021

Inactivation of caspase-8 is seen in NB [6,7] and mediates resistance to TRAIL (tumour necrosis factor-related apoptosis inducing ligand)-induced apoptosis [8]. Bcl-2 (b-cell CLL/lymphoma 2), an apoptotic suppressor, is expressed at high levels in many NBs [9,10] and is believed to prevent early apoptotic events in neuroblasts [11]. Some researchers have shown that the determination of Bcl-2 protein also provides prognostic information [10,12,13], while others have found no correlation between Bcl-2 oncoprotein expression and the clinical features of NB [9,14,15]. High expression of survivin, a family member of the inhibitor of apoptosis proteins (IAPs) localised to the 17q gain region, has also been shown to correlate with advanced stages of NB [16,17]. Moreover, the genes encoding caspase-1, caspase-9 and DFF45 have all been shown to be expressed to a low extent in advanced tumour stages [18–20].

In addition to inactivation of apoptotic pathways, constitutive survival signalling can inhibit apoptosis. Expression of different neurotrophin receptors of the tyrosine kinase (Trk) family plays an important role in the biology and clinical behaviour of NBs. Observations from several independent studies suggest that high expression of TrkA (encoded by *NTRK1*, neurotrophic tyrosine kinase receptor type 1) is present in NB with favourable biological features and highly correlated with patient survival, whereas TrkB is mainly expressed in unfavourable, aggressive NB with *MYCN*-amplification [21,22]. Activation of TrkA by its ligand nerve growth factor (NGF) initiates a cascade of signalling events and promotes neuronal differentiation *in vitro*. Activation of TrkB by its ligand brain-derived neurotrophic factor (BDNF) has been associated with proliferation and survival of NB cells (reviewed in Ref. [21]). Other growth factors essential for the maintenance of the peripheral nervous system are the fibroblast growth factor (FGF) and the insulin-like growth factors 1 and 2 (IGF-1, IGF-2; [23]. The NB cell line, SH-SY5Y, expresses both the type I and II IGF receptors [24] and secretes active IGF-2 [25] which promotes autocrine growth via the type I IGF receptor [26,27]. Neuronal growth is associated with increased IGF-2 mRNA and protein, whereas decreased IGF-2 mRNA and protein result in growth arrest [25,27].

Still, there are many important apoptotic mediators whose involvement in NB progression has not yet been investigated. Therefore, the aim of this study was to identify mRNA transcripts of genes involved in the apoptotic pathway, differentially expressed in NB tumours with favourable *versus* unfavourable biology. In this study, we screened cDNA expression filters containing 198 apoptotic factors for differentially expressed genes in two groups of clinical NB stages. The expression data were studied further using real-time reverse-transcriptase-polymerase chain reaction (RT-PCR). The results suggest that many apoptotic factors are downregulated in NB tumours with unfavourable biology which lead to suppression, primarily of the mitochondrial apoptotic pathway.

2. Materials and methods

2.1. Sample preparation

Tumour samples were obtained fresh frozen at surgery from 19 Scandinavian patients with diagnosed NB (Table 1; [28,29]). The patients were staged according to the International Neuroblastoma Staging System criteria (INSS; [30]). Total RNA was extracted from tumour samples using the RNeasy mini kit (QIAGEN, Hilden, Germany) or Totally RNA (Ambion, St. Austin, TX), according to the suppliers' protocols. When using the RNeasy mini kit, an additional DNase step was added (QIAGEN). Total RNA obtained from 3 normal control individuals was extracted from lymphocytes (ethylenediaminetetra-acetic-acid (EDTA) blood), enriched by Histopaque™ fractionation (Sigma–Aldrich Corporation, St. Louis, MO) and purified using RNA STAT-60 (Tel-Test, Friendswood, TX). The total RNA quality was evaluated by spectrophotometric analysis (wavelengths 260 and 280 nm) and by electrophoresis on a native 1% agarose w/v gel. All RNA samples showed an $A_{260}/A_{280\text{nm}}$ ratio in the range of 1.9–2.1, and both the 28S (at approximately 2 kb) and the 18S (at approximately 0.9 kb) ribosomal RNA bands were clearly visible on the gel.

2.2. Experimental design

In this study, tumours were divided into two biologically based groups by the following criteria: Favourable; NB patient with no evidence of disease with a primary tumour staged 1–3 with no *MYCN*-amplification and no 1p-deletion. Unfavourable; NB patient with advanced stage of disease or dead of disease with a primary tumour staged 4, or with a primary tumour staged 3 with *MYCN*-amplification and 1p-deletion (Table 1).

To identify differentially expressed genes, cDNA array analysis was performed in a group of four favourable and four unfavourable NB tumours. Genes were selected using the criteria of a fold-change (ratio) between the groups (favourable *versus* unfavourable) of at least 2. The expression data was further studied using real-time RT-PCR in a new set of six favourable and five unfavourable NB tumours (Table 1).

2.3. cDNA filters-laboratory procedures

The commercially available Human Apoptosis Expression Array (R&D systems, Minneapolis, MN) represents a collection of 198 genes involved in apopto-

Table 1
Clinical data concerning primary neuroblastomas used in this study

Assay	Group	Case	Stage	1p-del	MYCN	17q gain	Ploidy	Outcome
cDNA filters	F	14F6	1	neg	neg	neg	3n	NED
	F	18F1	1	neg	neg	pos		NED
	F	18F5	1	neg				NED
	F	10S7	1	neg				?
	UF	10S2	4	pos		(pos)		DOD
	UF	12S9	4	pos/neg	pos			NED[a]
	UF	13S0	4	pos	pos	pos		DOD
	UF	15S3	4	neg/pos	neg	pos		DOD
Real-time RT-PCR	F	12F8	3		neg			NED
	F	15F3	3	neg	neg	neg	5n	NED
	F	18F8	2A	neg			4n	NED
	F	20S9	2	neg	neg			NED
	F	23S4	2	neg	neg		3n	NED
	F	25S9	2	neg	neg			NED
	UF	4F1	4	neg	neg	pos	2n	DOD
	UF	13S1	3	pos	pos	pos		DOD
	UF	16S4	3	neg/pos	pos	pos		NED[a]
	UF	17S2	4	neg	neg			DOD
	UF	28S8	4	neg	neg			?

Column 2: F, favourable; UF, unfavourable; column 5–7: 1p del, 1p-deletion; MYCN, MYCN- amplification; 17q gain (according to Abel *et al*. [29]), neg, negative; pos, positive; (pos), uncertain results; neg/pos, ambiguous results based upon short tandem repeat polymorphism (according to Martinsson *et al*. [28]) and fluorescent *in situ* hybridisation (FISH); empty cells, not determined; column 9: NED, no evidence of disease; DOD, dead of disease.

[a] NED, these cases have unfavourable biological markers, but have been subjected to extensive therapy and have no evidence of disease.

sis, including pro- and anti-apoptotic factors, cell-cycle regulators, caspases, signal transduction factors, cytokines and their receptors, and other factors involved in apoptosis. The array consists of 206 different cloned cDNAs, printed as PCR products in duplicate on a nylon filter. Of these, eight are positive controls (housekeeping genes), and another six negative controls (empty vector) are also included in the array. Total RNA (2 μg) from eight NB tumours were annealed to apoptosis-specific primers (4 μl; R&D systems) in a sterile water-adjusted reaction volume of 15 μl on a thermal cycler at 90 °C for 2 min and were left to cool slowly to 42 °C. The RNA templates were labelled with ^{33}P in a RT-PCR containing 1× Reverse Transcriptase buffer, 333 μM each of deoxyadenosine triphosphate (dATP), deoxyguanidine triphosphate (dGTP), deoxythymidine triphosphate (dTTP), 1.67 μM deoxycytidine triphosphate (dCTP), 20 U RNasin, 20 μCi [α-^{33}P]dCTP, and 50U AMV Reverse Transcriptase. The solutions were adjusted with sterile water to a final reaction volume of 30 μl, and were incubated at 42 °C for an additional 2–3 h on a thermal cycler. Unincorporated radioactive nucleotides were removed from the labelling reaction in Sephadex G-25 spin columns (R&D-systems), and the percentage incorporation into the cDNA was roughly estimated using a hand-held Geiger–Mueller counter. Only cDNA with >50% incorporation were hybridised to the cDNA nylon filter. Hybridisations and washing steps were performed in roller bottles in a hybridisation oven at 65 °C, according to the suppliers' protocol. All samples were hybridised overnight (12–18 h). The cDNA arrays were exposed to a Kodak Low Energy Storage Phosphor Screen HD (Molecular Dynamics, Sunnyvale, CA) for 5–6 days and the imaging screens were scanned at 50 μm pixel size on a Molecular Imager FX Pro MultiImager System (BioRad Laboratories, Hercules, CA). All tumours were hybridised to two independent filters in two independent experiments.

2.4. cDNA filters-data analysis

Gene expression image files were exported as lineage TIFF files. Quantification and evaluation of gene expression signals were determined using the ArrayVision software (Imaging Research, Ontario, Canada). Pixel intensity of each spot was measured using the artefact removed mean (ARM) density parameter, in which pixels with density values that exceed four median absolute deviations (MADs) above the median are removed before the average of all pixels are calculated. Background was subtracted from each spot using the area below each spot group. The intensity of each spot was normalised using the average of all spots on the same filter as a reference, and the expression level was represented by the mean normalised intensity from the pair of duplicate spots. A comparative expression analysis was performed between all NB cases, presented as fold-change ratios between the samples. The logarithms of normalised expression levels were calculated, and compared with a two-sample *t*-test reporting two-tailed *P*-values.

Table 2
Summary of TaqMan data

Gene	Assay	Probe no.	Accession no.	Exon boundary	Assay location	Gene localisation	Group	Nominal *P*-value array	Nominal *P*-value real-time	Corrected *P*-value real-time	Combined nominal *P*-value
IL2RA	On demand	Hs00166229_m1	NM_000417	1/2	nt 223	10p15.1	Up	0.022*	0.067	0.54	0.0099**
MCL1	On demand	Hs00172036_m1	NM_021960	?	nt 823	1q21.2	Up	0.37	0.081	0.57	0.12
CDKN1A (P21)	On demand	Hs00355782_m1	NM_078467	2/3	nt 679	6p21.31	Up	0.0087**	0.13	0.78	0.0074**
IGF2	On demand	Hs00171254_m1	NM_000612	1/2	nt 550	11p15.5	Up	0.093	0.24	1	0.1
TRAF2	On demand	Hs00184192_m1	NM_021138	6/7	nt 661	9q34.3	Up	0.0082**	0.58	1	0.039*
DNCL1 (PIN)	by Design	185064448A 02	NM_003746	2/3	nt 225	12q24.31	Down	0.13	0.00049***	0.0054**	0.0012**
NTRK1 (TRKA)	On demand	Hs00176787_m1	NM_002529	3/4	nt 363	1q23.1	Down	0.0075**	0.0038**	0.039*	0.00059***
APAF1	On demand	Hs00185508_m1	NM_013229	?	nt 3141	12q23.1	Down	0.0061**	0.012*	0.11	0.001**
BAK1	by Design	185123495A 13	NM_001188	3/4	nt 417	6p21.31	Down	0.052	0.27	1	0.072
LTA (TNFB)	On demand	Hs00236874_m1	NM_000595	3/4	nt 350	6p21.33	Down	0.013*	0.3	1	0.024*
CASP7	On demand	Hs00169152_m1	NM_001227	6/7	nt 995	10q25.3	Down	0.040*	0.38	1	0.085
BID	On demand	Hs0060930_m1	NM_001196	2/3	nt 152	22q11.21	mito	0.16	0.0055**	0.055	0.0049**
BCL2	On demand	Hs00608023_m1	NM_000633	1/2	nt 616	18q21.33	mito	0.083	0.0061**	0.055	0.0032**
CASP9	On demand	Hs0060941_m1	NM_001229	2/3	nt 515	1p36.13–1p36.21	mito	0.480	0.015*	0.12	0.027*
CASP3	On demand	Hs00263337_m1	NM_032991	6/7	nt 668	4q35.1	mito	0.29	0.017*	0.12	0.018*
CASP2	On demand	Hs00154242_m1	NM_001224	6/7	nt 742	7q34	mito	0.044*	0.026*	0.15	0.0054**
BAD	On demand	Hs00188930_m1	NM_004322	1/2	nt 429	11q13.1	mito	0.097	0.17	0.85	0.83
BAX	On demand	Hs00751844_m1	NM_138762	?	nt 143	19q13.33	mito	nd	0.41	1	nd
BCL2L1 (BCLX)	On demand	Hs00236329_m1	NM_138578	2/3	nt 929	20q11.21	mito	0.82	0.67	1	0.67
CASP10	On demand	Hs00609648_m1	NM_032976	1/2	nt 185	2q33.1	mito	nd	0.73	1	nd
CASP8	On demand	Hs00154256_m1	NM_001228	6/7	nt 905	2q33.1	mito	0.065	0.97	1	0.17

Column 6: nt, nucleotide; Column 8: up, upregulated in unfavourable NB tumors on cDNA array; down, downregulated in unfavourable NB tumors on cDNA array; mito, mitochondrial involvement; Column 9: Nominal two-tailed *P*-values reported from relative expression in cDNA array analysis; Column 10: Nominal *P*-values reported from relative expression in real-time RT-PCR TaqMan analysis. The up and down groups report one-tailed *P*-values, and the mito-group reports two-tailed *P*-values; Column 11: *P*-values from column 10 corrected by Stepdown Bonferroni; Column 12: Nominal two-tailed *P*-values reported from combined cDNA array and TaqMan analysis. *BAX* and *CASP10* (nd, not determined) were both excluded from the cDNA array analysis because of very weak spot signals (see text for details). Statistical significance is marked: $*P < 0.05$, $**P < 0.01$, $***P < 0.001$.

2.5. Real-time RT-PCR – cDNA preparation

2.4 μg total RNA of each sample (12 μl) were reverse-transcribed in a 20 μl reaction containing 12.5 ng/μl Random Primers (Promega, Madison, WI), 0.5 mM deoxynucleotide triphosphate (dNTP)-mix (Amersham Pharmacia Biotech), 10 mM dithiothreitol (DTT), 1× First Strand Buffer, and 10 U Superscript II RNase H Reverse Transcriptase (Invitrogen, Carlsbad, CA). The samples were incubated at 25 °C for 10 min, reverse-transcribed at 42 °C for 50 min, followed by an inactivation step at 70 °C for 15 min.

2.6. Real-time RT-PCR – endogenous control

We used the TaqMan Human Endogenous Control Plate (Applied Biosystems, Foster City, CA) to select the most appropriate endogenous control for the real-time RT-PCR quantification analysis. Eight different samples of primary NB in different stages were tested for their expression levels of 10 commonly used housekeeping genes, *i.e.*, acidic ribosomal protein, β-actin, cyclophilin, glyceraldehyde-3-phosphate dehydrogenase, phosphoglycerokinase, β_2-microglobulin, β-glucuronidase, hypoxanthine ribosyl transferase, transcription factor IID (TATA binding protein), and transferrin receptor. The total RNA quantity in each sample was determined by spectrophotometric analysis at a wavelength of 260 nm. Real-time RT-PCR was performed in 96-well plates using a ABI PRISM® 7700 Sequence Detection System (Applied Biosystems). Amplification reactions (50 μl) were carried out in duplicate with 0.2 μl template cDNA, 1× TaqMan Universal PCR Master Mix (Applied Biosystems), 1× VIC-labelled Gene expression Assay Mix (pre-dried in wells), according to the suppliers' protocol (Applied Biosystems). Thermal cycling was initiated with a 2 min incubation at 50 °C, followed by a first denaturation step of 10 min at 95 °C, and then by 45 cycles of 15 s at 95 °C and 1 min at 60 °C. The ΔC_T (compared to a calibrator C_T) of each sample was calculated (data are available upon request).

2.7. Real-time RT-PCR with TaqMan

Real-time RT-PCR was performed in 384-well plates using a ABI PRISM® 7900HT Sequence Detection System (Applied Biosystems). TaqMan primers and probes (Table 2) were derived from the commercially available "TaqMan® Assays-on-Demand™ Gene Expression Products" (http://myscience.appliedbiosystems.com). A keyword search for each gene name or accession number was performed, and the respective assay kit was ordered directly from the website. If the gene in question was not available as Assays-on-Demand, we used the "Taqman® Assays-by-DesignSM Gene Expression Service" facility (Applied Biosystems). A selected part of the cDNA sequence, followed by information about exon–exon boundary sites, was uploaded to the website using the program File Builder (Applied Biosystems), and the best primer-probe set design was manufactured. Amplification reactions (10 μl) were carried out in duplicate with 0.1 μl of template cDNA, 1× TaqMan Universal PCR Master Mix (Applied Biosystems), 1× FAM-labelled Assay-on-Demand Gene expression Assay Mix (Applied Biosystems; Table 2). Thermal cycling was initiated with a 2 min incubation at 50 °C, followed by a first denaturation step of 10 min at 95 °C, and then by 40–50 cycles of 15 s at 95 °C and 1 min at 60 °C. In each assay, a standard curve with seven cDNA dilutions was recorded, and four no-template controls were included.

2.8. Real-time RT-PCR – quantification and normalisation

Quantification was performed by the standard-curve method. In summary, a standard curve was recorded in each PCR assay for all genes using serial dilutions (1:2.5, 1:5, 1:10, 1:20, 1:40, 1:80, 1:160) of calibrator cDNA (NB cell line IMR-32 or from normal blood). The mean C_T-value for duplicates were calculated, and the gene concentration (or gene copy number) of test samples were interpolated, based on standard curves. Standard curve dilutions were estimated to correspond to approximately 12, 6, 3, 1.5, 0.75, 0.375, 0.1875 ng/μl of the original total RNA. All samples were normalised to the housekeeping gene *GUSB* (β-glucuronidase) in the same cDNA sample.

2.9. Real-time RT-PCR – data analysis

The logarithms of expression levels were calculated and genes were compared with a two-sample *t*-test. Genes that were followed up by real-time RT-PCR were analysed in two groups: a confirmation group of 11 genes (up or down, Table 2) reporting one-tailed *P*-values, and a group of 10 genes, selected for its role in the mitochondrial pathway, reporting two-tailed *P*-values (Table 2). The *P*-values of the relative expression levels were corrected (P_c) by Step-down Bonferroni [31] for each group. In addition, a combined analysis (P_{comb}) of the *t*-statistic from the two experiments was performed by taking $t_{combined} = \sqrt{5}t_{microarray} + \sqrt{6}t_{taqman}$, where the weights are chosen to contribute equally to variance.

3. Results

3.1. cDNA filters

Sixty-seven of 206 genes (33%) were excluded from the analysis. Of these, 59 yielded a very weak or no

signal (generally a normalised ARM intensity < 0.1). In addition, all eight housekeeping genes were also excluded, since they were not considered to be of interest. The two independent filters from each tumour showed almost identical patterns (data not shown). The better of the two filters from each tumour was selected and the fold-change (ratio) in each tumour with unfavourable biology *versus* the average intensity in all tumours with favourable biology was determined (Table 1; Fig. 1). A calculation of the fold-change between groups (F and UF, Table 1) was also determined, based upon the average intensity in each group. Eleven differentially expressed genes were selected (Fig. 1(b)). Of these, *TRAF2*, *CDKN1A*, *IL2RA*, *IGF2*, *APAF1*, *NTRK1*, *LTA*, *CASP7*, *BAK* were differentially expressed by a factor exceeding 2.0 (ratio > 2.0), calculated by the average intensities between groups, and *MCL1* and *DNCL1* were differentially expressed by a factor exceeding 2.5 (ratio > 2.5) in two comparisons of a tumour with unfavourable biology *versus* the average of NB tumours with favourable biology (Fig. 1(b)). Of the selected genes, *TRAF2*, *CDKN1A*, *IL2RA*, *APAF1*, *NTRK1*, *LTA*, and *CASP7* correlated significantly ($P < 0.05$; Fig. 1(b)) after cDNA array data analysis. All selected genes were further analysed for verification by real-time RT-PCR.

3.2. Real-time RT-PCR

In order to select the most appropriate endogenous control for the real-time RT-PCR quantification analysis, we tested eight different primary NB samples in different stages for their expression levels of 10 commonly used housekeeping genes. *GUSB* (β-glucuronidase) and *B2M* (β_2-microglobulin) showed the lowest variations in ΔC_T levels, and were expressed at constant levels in all samples regardless of the NB stage (data are available on request). *GUSB* was selected, and used as an internal reference for normalisation in the real-time RT-PCR quantification analysis.

The 11 genes selected according to cDNA array analysis were validated by real-time RT-PCR in three tumours (cases 10S2, 13S0, 15S3) from the same initial tumour set (Table 1). These cases all showed nice correlations between the cDNA array and real-time RT-PCR assays. Unfortunately, no more material was available

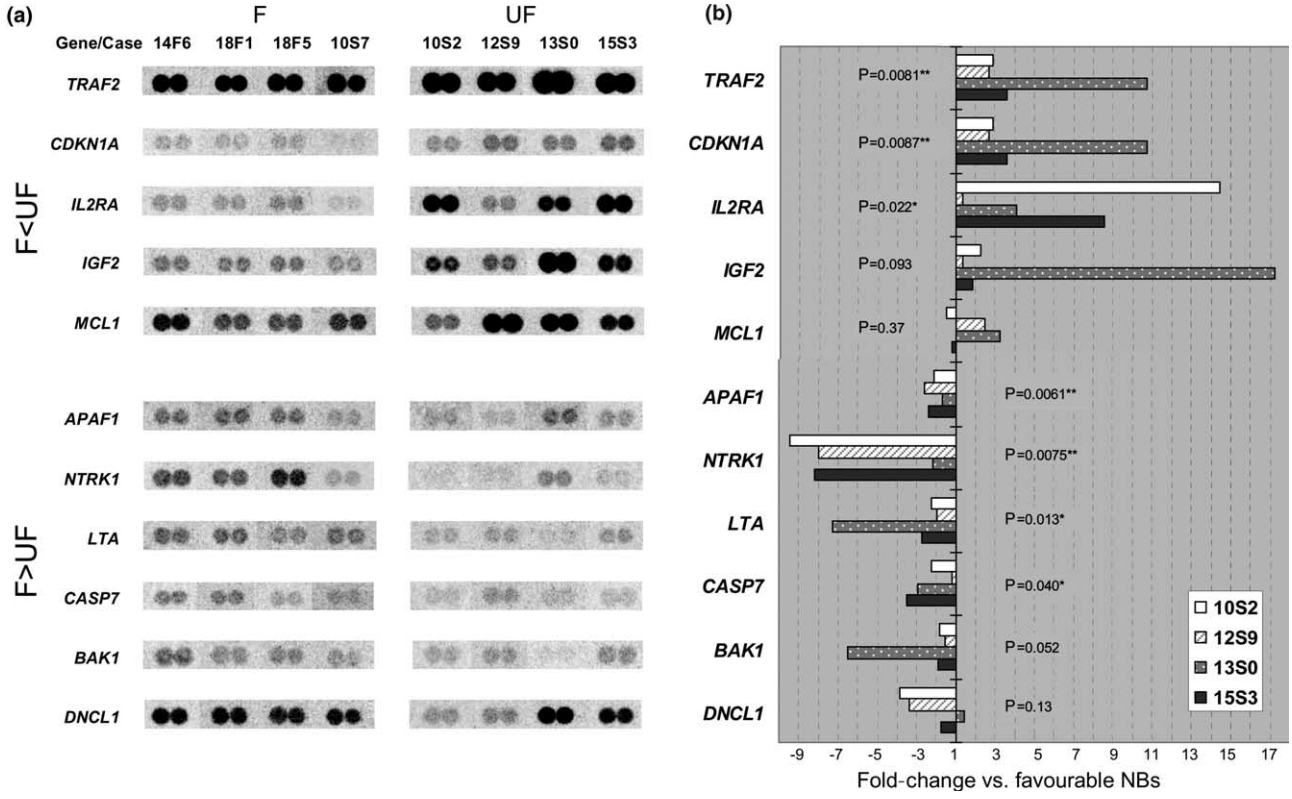

Fig. 1. Eleven differentially expressed genes studied by cDNA array analysis. (a) Array spot signals from four tumours with favourable biology (F, stage 1) and four tumours with unfavourable biology (UF, stage 4, Table 1). Upper panel; five genes preferentially expressed in tumours with unfavourable biology (F < UF). Lower panel; six genes preferentially expressed in tumours with favourable biology (F > UF). Signals are from image TIFF files generated after scanning of Phosphoimager screens exposed to each filter. (b) Diagram showing fold-change, upregulation (+) or downregulation (−), in each of four tumours with unfavourable biology (case: 10S2, 12S9, 13S0, and 15S3), *versus* the average intensity of four tumours with favourable biology (14F6, 18F1, 18F5, 10F7, stage 1; Table 1). Statistical significance is marked: *$P < 0.05$; **$P < 0.01$ (Table 2).

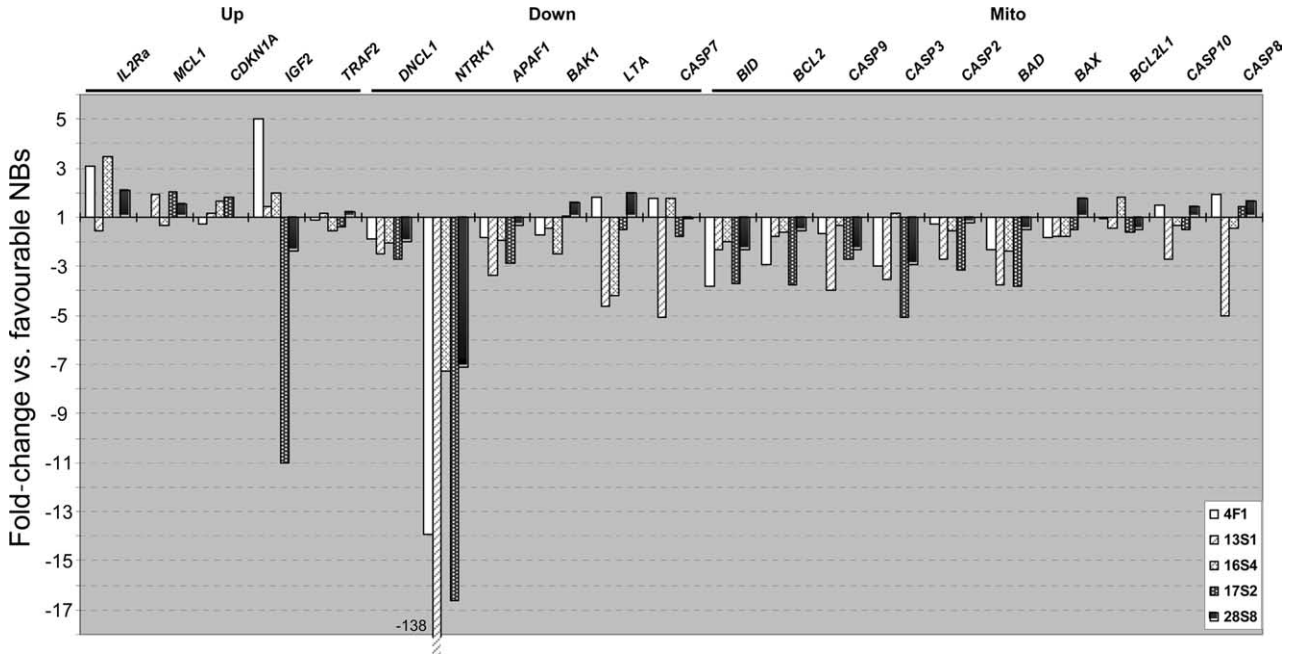

Fig. 2. Diagram showing fold-change, upregulation (+) or downregulation (−), of 21 genes analysed by real-time RT-PCR expression analysis. Six tumours with favourable biology and five tumours with unfavourable biology (Table 1) were analysed. Expression ratios were calculated in each tumour with unfavourable biology *versus* the average gene concentration in the six tumours with favourable biology. Up; genes selected from the cDNA array expressed to a high extent in tumours with unfavourable biology (Table 2). Down; genes selected from the cDNA array expressed to a low extent in tumours with unfavourable biology (Table 2). Mito; genes selected because of their involvement in the mitochondrial pathway (Table 2). A 138-fold decrease of *NTRK1* mRNA was found in case 13S1.

from the other five NB tumours from the initial tumour set, and these could therefore not be investigated by real-time RT-PCR. All 11 differentially expressed genes selected from the cDNA array were further analysed by real-time RT-PCR in a new set of six tumours with favourable and five tumours with unfavourable biology (Table 1; Fig. 2). Four mRNA transcripts (*MCL1*, *APAF1*, *CASP7*, and *BAK1*) encode proteins involved in the mitochondrial pathway of apoptosis. This prompted us to extend our real-time RT-PCR analysis to include 10 other genes encoding important mediators of this pathway (five caspases and five Bcl-2 family members; Table 2; Fig. 3). Significantly lower levels of *DNCL1* ($P_c = 0.0054$; Table 2) and *NTRK1* ($P_c = 0.039$) mRNA could be detected in NB tumours with unfavourable biology. *APAF1* ($P = 0.012$) was also found to be expressed to a low extent in NB tumours with unfavourable biology, and correlated significantly based upon the nominal *P*-value. *MCL1* ($P = 0.081$) was expressed to a high extent in some tumours of unfavourable biology (Fig. 2 and Table 2). mRNA transcripts encoded by *TRAF2*, *BAK1*, and *CASP7* could not be verified by real-time RT-PCR analysis (Fig. 2 and Table 2). Of the genes selected as a result of their involvement in the mitochondrial pathway, *BID* ($P = 0.055$) and *BCL2* ($P = 0.055$; Table 2) showed apparently lower mRNA levels in tumours in advanced stages, compared with those with favourable biology. *CASP2*, *3*, and *9* were also expressed to a lower extent in tumours with unfavourable biology and correlated significantly according to nominal *P*-values ($P < 0.05$), following real-time RT-PCR analysis.

3.3. Combined data analysis

The combined data analysis of microarray and real-time RT-PCR suggest the mRNA level of *IL2RA* ($P_{comb} = 0.0099$) and *CDKN1A* ($P_{comb} = 0.0074$; Table 2) to be upregulated in tumours with unfavourable biology. In addition, *APAF1* ($P_{comb} = 0.001$) *CASP2* ($P_{comb} = 0.0054$), *CASP3* ($P_{comb} = 0.018$), and *CASP9* ($P_{comb} = 0.027$) were found to be downregulated in NB tumours with unfavourable biology. Moreover, *LTA* ($P_{comb} = 0.024$) was found to be expressed to a lower extent in some NB tumours in advanced stages, but this could not be verified by real-time RT-PCR analysis ($P = 0.3$, Table 2).

4. Discussion

In the search for a tumour suppressor gene proposed to be inactivated in advanced stages of NB tumours, we and others have been searching for mutations in several candidate genes, with a focus on the heterozygously deleted area on the distal part of chromosome arm 1p [32].

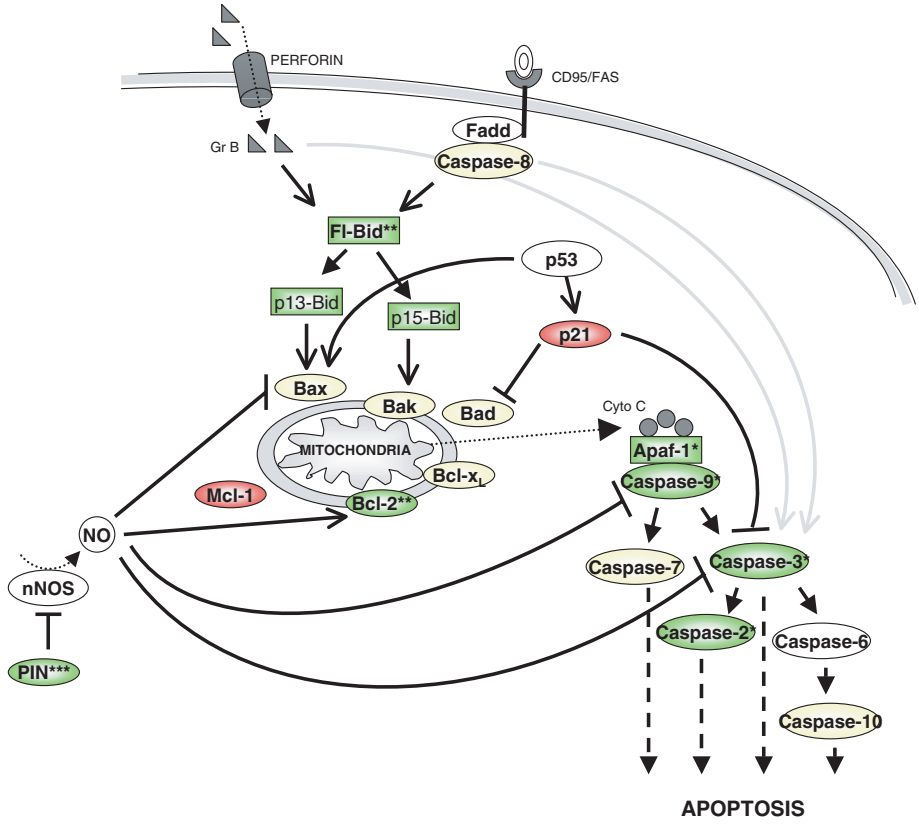

Fig. 3. Simplified schematic representation of apoptosis focused mainly on the mitochondrial apoptotic pathway. Intracellular stimuli induce the activation involving proteins of the Bcl-2 family, *i.e.* Bid, Bad, Bax, Bak (pro-apoptotic), and Bcl-2, Bcl-x, Mcl-1 (anti-apoptotic), which results in alteration of the permeability of the mitochondrial membrane. Cytochrome *c* migrates from the intermembrane space into the cytosol and interacts with the Apaf-1 protein. The resulting complex activates caspase-9 and, in turn, caspase-3. Activated caspase-3 causes the final apoptotic event. Several transcripts, encoding proteins involved in this pathway, are shown in Fig. 2 to be differentially expressed in tumours with unfavourable *versus* tumours with favourable biology in this study. Proteins expressed to a lower extent in tumours with unfavourable compared with those with favourable biology (Apaf-1, caspase-2, PIN, Bcl-2, Bid, caspase-3, caspase-9), are marked in green, proteins expressed to a higher extent in tumours with unfavourable compared with those with favourable biology (p21 and Mcl-1) are marked in red, and genes checked by real-time RT-PCR expressed uniformly in NB tumours of all stages are marked in yellow. Statistical significance is marked: $*P < 0.05$, $**P < 0.01$ (Table 2). See text for more details.

Recently, we found some rare allele variants in two genes located in 1p36, one encoding the alpha subunit of the DNA Fragmentation Factor (DFF45), and the other encoding caspase-9, a key caspase in the mitochondrial pathway [19]. A number of publications reveal a correlation between apoptotic factors and the prognosis of NB patients [6–13,16,17,19,20]. In an attempt to investigate the role of aberrant apoptosis in NB progression, we have now screened an apoptotic cDNA array in order to find genes that are differentially expressed in tumours with unfavourable *versus* favourable biology. Our intention was to investigate the expression level of individual apoptotic genes, as well as to look at mRNA levels of proteins in the apoptotic pathway as a whole, in NB tumours with different biological characteristics.

4.1. The Bcl-2 family members

Cytochrome *c* release is a critical step in the activation of the downstream caspase protease cascade [33]. The anti-apoptotic members, Bcl-2, Bcl-x_L (bcl-2 like 1), and Mcl-1 (myeloid cell leukaemia sequence 1), all work by blocking cytochrome *c* release from mitochondria, whereas the pro-apoptotic members, Bid (BH3 interacting domain death agonist), Bad (bcl-2 antagonist of cell death), Bax (bcl-2-associated X protein), and Bak (bcl-2 antagonist killer), promote this release (Fig. 3). In contrast to the findings from many other studies [9,10,12,13], we found Bcl-2 ($P_c = 0.055$, Table 2) to be preferentially expressed in NB tumours with favourable biology (Fig. 2). This puzzling finding could be explained by the different techniques used to perform gene expression analysis in different studies. In all cited publications, Bcl-2 expression was detected by immunohistochemical analysis, a technique that allows individual cells to be studied and correlations to other prognostic markers can be made more easily. The mRNA stability of the *BCL2* transcript in treated and untreated NB patients is of course also a factor that should be taken into consideration. *BCL2* is localised to 18q21.33, a region

that displays a high frequency of allelic imbalance in advanced NB stages [34]. This feature could lead to the lower copy number in advanced tumours found in this study. However, according to Takita and colleagues [35], *BCL2* is localised outside of the most commonly deleted region in 18q21.1.

In contrast to *BCL2*, the gene encoding myeloid cell leukaemia sequence 1 (*MCL1*) is upregulated in some advanced NB stages (Figs. 1 and 2). Mcl-1 has been shown to prolong cell viability and, like Bcl-2, to interact with Bax [36,37]. Genetically engineered mice with *MYCN* overexpression targeted to cells derived from the neural crest using the tyrosine hydroxylase promoter have been shown to develop NB several months after birth. Interestingly, a comparative genomic hybridisation (CGH) analysis of the resulting murine NBs reveals gain of the murine Mcl-1 locus in up to 56% of tumours [38,39].

Bad works through inhibition of the mitochondrial membrane-associated partners, Bcl-2 and Bcl-x_L, by complex formation [33]. Bad is rapidly phosphorylated in response to survival factors, which results in dissociation from Bcl-2 and Bcl-x_L complexes [40]. Using real-time RT-PCR analysis, slightly lower levels of *BAD* could be detected in NB tumours with unfavourable *versus* favourable biology (Fig. 2), while cDNA array analysis yielded uniform expression. Low levels of Bad would lead to decreased levels of cytochrome *c* release, decreased activation of the caspase cascade and apoptosis.

4.2. The cytotoxic and death receptor pathways

Experiments have shown that the Fas/caspase-8 death receptor pathway is coupled to the mitochondrial pathway through the pro-apoptotic protein Bid ([41,42]; Fig. 3). Both the cytotoxic (directly, through granzyme B, GrB) and the death receptor pathways (indirectly, through caspase-8) induce apoptosis mainly through the proteolytic cleavage of full-length Bid (Fl-Bid), resulting in two different proteolytic truncations of Bid (p13-tBid and p15-tBid), respectively ([43]; Fig. 3). These proteolytic truncations exhibit different affinities towards Bax and Bak. Moreover, Bax and Bak have been shown to play a non-redundant role in Bid-mediated apoptosis, as double Bax and Bak deficiency severely impairs the apoptotic programme [43]. Although *BAK1* was found to be downregulated in tumours with unfavourable biology using cDNA array analysis, we concluded from the real-time RT-PCR analysis that the genes encoding both Bax and Bak were uniformly expressed, irrespective of tumour biology. However, the low level of *BID* mRNA ($P_c = 0.055$; Table 2) in NB tumours with unfavourable biology would affect the cross-talk of the cytotoxic and death receptor pathways with the mitochondrial pathway appreciably and, at least to some extent, yield the same effect as double Bax and Bak deficiency (Fig. 3).

Caspase-8 has been shown to be silenced by DNA methylation, as well as by gene deletion, in NB tumours with unfavourable biology [6,7]. Using cDNA array analysis, we found the *CASP8* mRNA level to be half as much in tumours with unfavourable biology as in NB tumours with favourable biology ($P = 0.065$, ratio 1.7, data not shown). However, this could not be verified by real-time RT-PCR analysis, through which low levels of *CASP8* mRNA were found only in case 13S1 (Fig. 2).

4.3. P53-induced apoptosis

DNA damage and oxidative stress activate two pathways, one involving p53-dependent apoptosis through transcriptional upregulation of Bax, and the other involving p53-dependent activation of p21 that protects cells from apoptosis ([44]; Fig. 3). p21, encoded by *CDKN1A* (cyclin-dependent kinase inhibitor 1A), is a major inhibitor of p53-dependent and p53-independent apoptosis, and may block apoptosis by interacting with pro-apoptotic molecules such as procaspase-3 and caspase-8. Moreover, the p21-activated kinase 5 (Pak5) has been shown to inhibit apoptosis by phosphorylating Bad [45]. Although not significantly verified by real-time RT-PCR, the combined data analysis indicates *CDKN1A* ($P_{comb} = 0.0074$; Table 2) to be upregulated in advanced tumour stages (Figs. 1(b) and 2). However, p21 may possess both pro-apoptotic and anti-apoptotic abilities, depending on the specific cellular context [46].

4.4. The caspase cascade

Oligomeric Apaf-1 (apoptotic protease activating factor 1) mediates cytochrome *c*-dependent autocatalytic activation of procaspase-9, thereby initiating the proteolytic cascade that culminates in apoptosis (Fig. 3). In this study, we found the genes encoding Apaf-1 and caspase-9 to be expressed to a low extent in tumours from patients with an unfavourable biology. This confirms an earlier study, in which we found lower expression levels of *CASP9* in advanced staged NB tumours, compared with NB tumours with favourable biology, detected by RT-PCR in primary NBs [19]. In contrast, Apaf-1 and caspase-9 have been shown to be expressed and functionally active in human NB cell lines with 1p36 loss of heterozygosity (LOH) and amplified *MYCN*. Interestingly, caspase-9 has been shown to be a necessary response to the cytotoxic drugs doxorubicin and cisplatin, whereas caspase-8 is not activated and blocking of its function does not interfere within drug-treated cells [47].

All ''executioner'' pathways of apoptosis cause the proteolytic activation of caspase-3 (and its homologues, caspase-6 and -7), followed by the final cascade with cleavage of multiple downstream substrates (Fig. 3).

We found that the mRNA level of caspase-3 (*CASP3*) is frequently downregulated in tumours with unfavourable compared with NB tumours with favourable biology. This confirms an earlier finding of caspase-3 deficiency in human NB [48]; a significant percentage of NB tumours were revealed to lack caspase-3 mRNA and protein. However, Iolascon and colleagues could not find any correlation between caspase-3 mRNA deficiency and tumour stage or *MYCN* status [48]. We also found a decreased copy number of the downstream caspase-2 in advanced tumour stages, whereas caspase-7 and caspase-10 were found to be uniformly expressed in all tumour stages (Fig. 2).

4.5. Survival signalling

Nitric oxide (NO) has been shown to play a neuroprotective role both in the NB cell line SH-SY5Y [49] and in dorsal root ganglion neurons [50], by inhibiting Bax, caspase-3 and caspase-9 ([50]; Fig. 3). Moreover, Ciani and colleagues found that Bcl-2 is downregulated in cerebellar neurons by NO shortage [51]. PIN (protein inhibitor of neuronal nitric oxide synthase) or DLC1 (dynein light chain) is an integral component of the dynein motor complex and is known to physically interact with and inhibit the activity of neuronal nitric oxide synthase (nNOS; Fig. 3). We found the mRNA transcript (*DNCL1*, dynein cytoplasmic light polypeptide 1) encoding PIN to be significantly ($P_c = 0.0054$) downregulated in tumours from patients who died from disease progression, which would lead to higher levels of NO, and thus to a higher degree of cell death inhibition in these cases.

Neurotrophin signalling plays a central role in normal neural development, and low expression of *NTRK1* (encoding TrkA) is a well known prognostic marker of advanced stages of NBs [21,52]. These observations were further supported by our data, in which *NTRK1* was shown to be significantly ($P_c = 0.030$) downregulated in all advanced tumour stages, compared with those with favourable biology. *NTRK1* was found to be decreased 2–8-fold in tumours with unfavourable biology using cDNA array analysis (Fig. 1(b)), and 7-138-fold in NB tumours with unfavourable biology analysed using real-time RT-PCR (Fig. 2).

IGF-2 is the major autocrine growth factor for NB. Neuronal growth is associated with increased IGF-2 mRNA and protein, and the NB cell line SH-SY5Y has been shown to establish an autocrine growth loop via IGF-2 secretion and the type I IGF receptor [26,27]. IGF-2 has also been suggested to counteract the effects of retinoic acid treatment [53]. In this study, we found IGF-2 to be expressed at high levels in some tumours with unfavourable biology by screening of the apoptotic cDNA filter (Fig. 1). However, this expression pattern could not be confirmed by real-time RT-PCR analysis (Fig. 2).

Interleukin-2 (IL-2) signalling is important in T-cell activation and proliferation following antigen-induced T-cell response. Synthesis of the alpha chain of the IL-2 receptor (encoded by *IL2RA*) as well as the cytokine IL-2 is induced in response to T-cell activation, and binding of IL-2 to its high affinity receptor promotes T-cell growth in an autocrine fashion. It is also speculated that IL-2 can engage in tumour-promoting activity in human non-haemapoietic cells [54]. High levels of the *IL2RA* transcript ($P_{comb} = 0.0099$; Table 2) were seen in some advanced staged NB tumours (Figs. 1 and 2). Unfortunately, the expression signal for *IL2* was considered to be too weak, and this gene could therefore not be included in the data analysis of the cDNA filters. Lymphotoxin (LT-α), also known as tumour necrosis factor-β (TNF-β), is a cytokine that binds in its homotrimeric form to Tnfr-1, Tnfr-2, and HVEM. LT-α is produced by lymphocytes and is cytotoxic to a wide range of tumour cells *in vitro* and *in vivo*. We detected low levels of *LTA* mRNA in some NB tumours with unfavourable biology (Figs. 1 and 2). Puzzlingly, *LTA* expression has been found to be positively regulated by IL-2 signalling via the Jak-STAT pathway in secondary lymphoid organs [55].

In summary, of the 21 transcripts analysed, several mRNA transcripts encoding pro-apoptotic mediators of the mitochondrial pathway were found, using real-time RT-PCR analysis, to be preferably expressed in NB tumours of the more favourable subtype. However, only the genes encoding PIN (*DNCL1*; $P_c < 0.05$) and TrkA (*NTRK1*; $P_c < 0.05$) were significantly downregulated, and the genes encoding Bcl-2 ($P_c = 0.055$) and Bid ($P_c = 0.055$) were evidently downregulated in tumours with unfavourable compared with tumours with favourable biology. The apparent imbalance between pro-apoptotic and anti-apoptotic mediators might have a decisive effect on the development and aggressive behaviour of advanced neuroblastoma. The specific downregulation of important regulators in the intrinsic caspase-dependent apoptotic pathway may be responsible for drug resistance in high-risk NB. As recently shown, the specific activation of the mitochondrial apoptotic pathway using cyclooxygenase-2 inhibitors effectively induces apoptosis of NB cells both *in vitro* and *in vivo* [56]. We conclude that our results should have significance with regard to the design of novel therapeutic approaches that specifically address the imbalance of the intrinsic apoptotic pathway in aggressive NB.

Conflict of interest statement

None declared.

Acknowledgement

We would like to thank the Swegene Gothenburg Genomics resource unit, for help and access to the ABI PRISM® 7900HT Sequence Detection System. This work was supported by grants from the Swedish Cancer Society, the Children's Cancer Foundation, the King Gustav V Jubilee Clinic Cancer Research Foundation, the Assar Gabrielsson Foundation, the Wilhelm and Martina Lundgren Research Foundation, the Nilsson-Ehle Foundation, and the Sahlgrenska University Foundation.

References

1. Brodeur GM. Neuroblastoma: Biological insights into a clinical enigma. *Nat Rev Cancer* 2003, **3**, 203–216.
2. Bown N, Cotterill S, Lastowska M, *et al*. Gain of chromosome arm 17q and adverse outcome in patients with neuroblastoma. *N Engl J Med* 1999, **340**, 1954–1961.
3. Maris JM, Guo C, Blake D, *et al*. Comprehensive analysis of chromosome 1p deletions in neuroblastoma. *Med Pediatr Oncol* 2001, **36**, 32–36.
4. Vaux DL, Haecker G, Strasser A. An evolutionary perspective on apoptosis. *Cell* 1994, **76**, 777–779.
5. Nagata S. Apoptosis by death factor. *Cell* 1997, **88**, 355–365.
6. Teitz T, Wei T, Valentine MB, *et al*. Caspase 8 is deleted or silenced preferentially in childhood neuroblastomas with amplification of MYCN [see comments]. *Nat Med* 2000, **6**, 529–535.
7. Teitz T, Lahti JM, Kidd VJ. Aggressive childhood neuroblastomas do not express caspase-8: an important component of programmed cell death. *J Mol Med* 2001, **79**, 428–436.
8. Hopkins-Donaldson S, Bodmer JL, Bourloud KB, *et al*. Loss of caspase-8 expression in highly malignant human neuroblastoma cells correlates with resistance to tumor necrosis factor-related apoptosis-inducing ligand-induced apoptosis. *Cancer Res* 2000, **60**, 4315–4319.
9. Ikeda H, Hirato J, Akami M, *et al*. Bcl-2 oncoprotein expression and apoptosis in neuroblastoma. *J Pediatr Surg* 1995, **30**, 805–808.
10. Mejia MC, Navarro S, Pellin A, Castel V, Llombart-Bosch A. Study of bcl-2 protein expression and the apoptosis phenomenon in neuroblastoma. *Anticancer Res* 1998, **18**, 801–806.
11. van Golen CM, Castle VP, Feldman EL. IGF-I receptor activation and BCL-2 overexpression prevent early apoptotic events in human neuroblastoma. *Cell Death Differ* 2000, **7**, 654–665.
12. Castle VP, Heidelberger KP, Bromberg J, *et al*. Expression of the apoptosis-suppressing protein bcl-2, in neuroblastoma is associated with unfavorable histology and N-myc amplification. *Am J Pathol* 1993, **143**, 1543–1550.
13. Oue T, Fukuzawa M, Kusafuka T, *et al*. In situ detection of DNA fragmentation and expression of bcl-2 in human neuroblastoma: relation to apoptosis and spontaneous regression. *J Pediatr Surg* 1996, **31**, 251–257.
14. Ikegaki N, Katsumata M, Tsujimoto Y, *et al*. Relationship between bcl-2 and myc gene expression in human neuroblastoma. *Cancer Lett* 1995, **91**, 161–168.
15. Ramani P, Lu QL. Expression of bcl-2 gene product in neuroblastoma. *J Pathol* 1994, **172**, 273–278.
16. Azuhata T, Scott D, Takamizawa S, *et al*. The inhibitor of apoptosis protein survivin is associated with high-risk behavior of neuroblastoma. *J Pediatr Surg* 2001, **36**, 1785–1791.
17. Islam A, Kageyama H, Takada N, *et al*. High expression of survivin, mapped to 17q25, is significantly associated with poor prognostic factors and promotes cell survival in human neuroblastoma. *Oncogene* 2000, **19**, 617–623.
18. Ohira M, Kageyama H, Mihara M, *et al*. Identification and characterization of a 500-kb homozygously deleted region at 1p36.2–p36.3 in a neuroblastoma cell line [In Process Citation]. *Oncogene* 2000, **19**, 4302–4307.
19. Abel F, Sjoberg RM, Ejeskar K, *et al*. Analyses of apoptotic regulators CASP9 and DFFA at 1P36.2, reveal rare allele variants in human neuroblastoma tumours. *Br J Cancer* 2002, **86**, 596–604.
20. Ikeda H, Nakamura Y, Hiwasa T, *et al*. Interleukin-1 beta converting enzyme (ICE) is preferentially expressed in neuroblastomas with favourable prognosis. *Eur J Cancer* 1997, **33**, 2081–2083.
21. Eggert A, Ikegaki N, Liu XG, *et al*. Prognostic and biological role of neurotrophin-receptor TrkA and TrkB in neuroblastoma. *Klin Padiatr* 2000, **212**, 200–205.
22. Kogner P, Barbany G, Dominici C, *et al*. Coexpression of messenger RNA for TRK protooncogene and low affinity nerve growth factor receptor in neuroblastoma with favorable prognosis. *Cancer Res* 1993, **53**, 2044–2050.
23. Prager D, Yamasaki H, Weber MM, *et al*. Role of the insulin-like growth factors in regulating neuroendocrine function. *Neurobiol Aging* 1994, **15**, 569–572.
24. Martin DM, Yee D, Carlson RO, *et al*. Gene expression of the insulin-like growth factors and their receptors in human neuroblastoma cell lines. *Brain Res Mol Brain Res* 1992, **15**, 241–246.
25. Martin DM, Feldman EL. Regulation of insulin-like growth factor-IL expression and its role in autocrine growth of human neuroblastoma cells. *J Cell Physiol* 1993, **155**, 290–300.
26. Martin DM, Singleton JR, Meghani MA, *et al*. IGF receptor function and regulation in autocrine human neuroblastoma cell growth. *Regul Pept* 1993, **48**, 225–232.
27. Meghani MA, Martin DM, Singleton JR, *et al*. Effects of serum and insulin-like growth factors on human neuroblastoma cell growth. *Regul Pept* 1993, **48**, 217–224.
28. Martinsson T, Sjoberg RM, Hedborg F, *et al*. Deletion of chromosome 1p loci and microsatellite instability in neuroblastomas analyzed with short-tandem repeat polymorphisms. *Cancer Res* 1995, **55**, 5681–5686.
29. Abel F, Ejeskar K, Kogner P, *et al*. Gain of chromosome arm 17q is associated with unfavourable prognosis in neuroblastoma, but does not involve mutations in the somatostatin receptor 2 (SSTR2) gene at 17q24. *Br J Cancer* 1999, **81**, 1402–1409.
30. Brodeur GM, Pritchard J, Berthold F, *et al*. Revisions of the international criteria for neuroblastoma diagnosis, staging, and response to treatment. *J Clin Oncol* 1993, **11**, 1466–1477.
31. Holm S. A simple sequentially rejective multiple test procedure. *Scand J Statist* 1979, **6**, 65–70.
32. Krona C, Ejeskar K, Abel F, *et al*. Screening for gene mutations in a 500 kb neuroblastoma tumor suppressor candidate region in chromosome 1p; mutation and stage-specific expression in UBE4B/UFD2. *Oncogene* 2003, **22**, 2343–2351.
33. Green DR, Reed JC. Mitochondria and apoptosis. *Science* 1998, **281**, 1309–1312.
34. Cunsolo CL, Bicocchi MP, Petti AR, *et al*. Numerical and structural aberrations in advanced neuroblastoma tumours by CGH analysis; survival correlates with chromosome 17 status. *Br J Cancer* 2000, **83**, 1295–1300.
35. Takita J, Hayashi Y, Takei K, *et al*. Allelic imbalance on chromosome 18 in neuroblastoma. *Eur J Cancer* 2000, **36**, 508–513.
36. Sato T, Hanada M, Bodrug S, *et al*. Interactions among members of the Bcl-2 protein family analyzed with a yeast two-hybrid system. *Proc Natl Acad Sci USA* 1994, **91**, 9238–9242.
37. Zhou P, Qian L, Kozopas KM, Craig RW. Mcl-1, a Bcl-2 family member, delays the death of hematopoietic cells under a variety of apoptosis-inducing conditions. *Blood* 1997, **89**, 630–643.

38. Weiss WA, Aldape K, Mohapatra G, *et al*. Targeted expression of MYCN causes neuroblastoma in transgenic mice. *EMBO J* 1997, **16**, 2985–2995.
39. Weiss WA, Godfrey T, Francisco C, *et al*. Genome-wide screen for allelic imbalance in a mouse model for neuroblastoma. *Cancer Res* 2000, **60**, 2483–2487.
40. Gajewski TF, Thompson CB. Apoptosis meets signal transduction: elimination of a BAD influence. *Cell* 1996, **87**, 589–592.
41. Li H, Zhu H, Xu CJ, Yuan J. Cleavage of BID by caspase 8 mediates the mitochondrial damage in the Fas pathway of apoptosis. *Cell* 1998, **94**, 491–501.
42. Luo X, Budihardjo I, Zou H, *et al*. Bid, a Bcl2 interacting protein, mediates cytochrome *c* release from mitochondria in response to activation of cell surface death receptors. *Cell* 1998, **94**, 481–490.
43. Cartron PF, Juin P, Oliver L, *et al*. Nonredundant role of Bax and Bak in Bid-mediated apoptosis. *Mol Cell Biol* 2003, **23**, 4701–4712.
44. Gartel AL, Tyner AL. The role of the cyclin-dependent kinase inhibitor p21 in apoptosis. *Mol Cancer Ther* 2002, **1**, 639–649.
45. Cotteret S, Jaffer ZM, Beeser A, *et al*. p21-Activated kinase 5 (Pak5) localizes to mitochondria and inhibits apoptosis by phosphorylating BAD. *Mol Cell Biol* 2003, **23**, 5526–5539.
46. Liu S, Bishop WR, Liu M. Differential effects of cell cycle regulatory protein p21(WAF1/Cip1) on apoptosis and sensitivity to cancer chemotherapy. *Drug Resist Updat* 2003, **6**, 183–195.
47. Bian X, Giordano TD, Lin HJ, *et al*. Chemotherapy-induced apoptosis of S-type neuroblastoma cells requires caspase-9 and is augmented by CD95/Fas stimulation. *J Biol Chem* 2004, **279**, 466–4669.
48. Iolascon A, Borriello A, Giordani L, *et al*. Caspase 3 and 8 deficiency in human neuroblastoma. *Cancer Genet Cytogenet* 2003, **146**, 41–47.
49. Andoh T, Lee SY, Chiueh CC. Preconditioning regulation of bcl-2 and p66shc by human NOS1 enhances tolerance to oxidative stress. *FASEB J* 2000, **14**, 2144–2146.
50. Thippeswamy T, McKay JS, Morris R. Bax and caspases are inhibited by endogenous nitric oxide in dorsal root ganglion neurons in vitro. *Eur J Neurosci* 2001, **14**, 1229–1236.
51. Ciani E, Guidi S, Bartesaghi R, Contestabile A. Nitric oxide regulates cGMP-dependent cAMP responsive element binding protein phosphorylation and Bcl-2 expression in cerebellar neurons: implication for a survival role of nitric oxide. *J Neurochem* 2002, **82**, 1282–1289.
52. Kogner P, Barbany G, Bjork O, *et al*. Trk mRNA and low affinity nerve growth factor receptor mRNA expression and triploid DNA content in favorable neuroblastoma tumors. *Prog Clin Biol Res* 1994, **385**, 137–145.
53. Melino G, Stephanou A, Annicchiarico-Petruzzelli M, *et al*. Modulation of IGF-2 expression during growth and differentiation of human neuroblastoma cells: retinoic acid may induce IGF-2. *Neurosci Lett* 1993, **151**, 187–191.
54. Azzarone B, Pottin-Clemenceau C, Krief P, *et al*. Are interleukin-2 and interleukin-15 tumor promoting factors for human non-hematopoietic cells. *Eur Cytokine Netw* 1996, **7**, 27–36.
55. Reddy J, Chastagner P, Fiette L, *et al*. IL-2-induced tumor necrosis factor (TNF)-beta expression: further analysis in the IL-2 knockout model, and comparison with TNF-alpha, lymphotoxin-beta, TNFR1 and TNFR2 modulation. *Int Immunol* 2001, **13**, 135–147.
56. Johnsen JI, Lindskog M, Ponthan F, *et al*. Cyclooxygenase-2 is expressed in neuroblastoma, and nonsteroidal anti-inflammatory drugs induce apoptosis and inhibit tumor growth in vivo. *Cancer Res* 2004, **64**, 7210–7215.